

Novel Quantum Phases of Ultracold Bosonic Atoms in Optical Superlattices

Jing-Min Hou*

Department of Physics, Southeast University, Nanjing, 211189, China

(Dated: May 14, 2007)

We study quantum phases of ultracold bosonic atoms in a two-dimensional optical superlattice. The extended Bose-Hubbard model derived from the system of ultracold bosonic atoms in an optical superlattice is solved numerically with Gutzwiller approach. We find that supersolid(SS), density-wave(DW) phases appear in some regimes of parameters, addition to Mott-insulator (MI) phase, while the superfluid phase, which conventionally appears in optical lattice-cold atom systems, is absent in this system. The experimental detection of the first order correlations and the second order correlations of different quantum phases with time-of-flight and noise-correlation techniques is proposed.

PACS numbers: 03.75.Lm, 03.75.Nt, 32.80.Pj

Ultracold atoms in optical lattices, which provide an intriguing environment to study strongly correlated condensed matter systems and quantum information due to the complete control over the system parameters, have been extensively investigated theoretically and experimentally. The superfluid-Mott-insulator transition of ultracold bosons in optical lattices has been theoretically analyzed and experimentally demonstrated[1, 2]. The realization of 1D quantum liquids with atomic gases has achieved[3]. A Bose spin glass of ultracold bosons in an optical lattice has been demonstrated[4]. Repulsively bound states in an optical lattice have been observed in a recent experiment[5]. Atomic Bose-Fermi mixtures in an optical lattice have been studied[8]. Ultracold fermionic atoms in optical lattices have also been investigated recently[6, 7]. Diverse schemes of quantum information processing in optical lattices have been proposed[9].

The existence of a supersolid phase between the quantum liquid and the quantum solid at zero temperature was proposed several decades ago[10]. Supersolid phase is an exotic quantum phase, in which the off-diagonal long range order (ODLRO) and the diagonal long-range order (DLRO) coexist. Recently such a supersolid phase has been observed in bulk solid ^4He in a seminal experiment by Kim and Chan[11]. Many efforts have also been made to search the supersolid phase in optical lattice-cold atom systems. Theoretical calculations suggest that the supersolid phase exists in the systems of cold bosons with dipolar interactions in an optical lattice[12], bosons confined to higher bands of optical lattice[13], 2D Bose-Fermi mixtures[14], and hard core bosons with the nearest-neighbor repulsion in a triangular lattice[15]. All of these systems require interactions beyond the on-site repulsion, *e.g.*, the nearest-neighbor interactions, which can arise from a long range dipolar interaction or a short-range interaction between bosons in higher bands of the lattice.

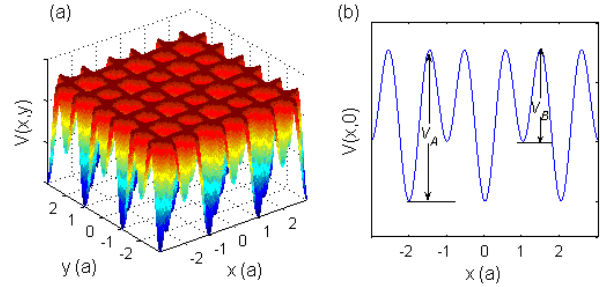


FIG. 1: (color online). (a) Schematic diagram of a two-dimensional optical superlattice potential, where x and y are coordinates in units of lattice constant a and $V(x,y)$ represents the potential energy at position (x,y) . (b) The profile of the optical superlattice potential shown in (a) at $y=0$. Here V_A and V_B represent the lattice depths of the sublattices A and B respectively.

In this Letter, we will study the system of ultracold bosonic atoms in a two-dimensional optical superlattice *without the nearest-neighbor interactions*. We will show that novel quantum phases, such as supersolid, density wave, and Mott-insulator phases, appear in some regimes of quantum parameters. We will display the first order correlation function and the second order correlation function in the lattice momentum space for different quantum phases in order to identify them in experiments with the time-of-flight and noise-correlation techniques.

Ultracold bosons with repulsive interactions in an external potential can be described by a second quantized Hamiltonian as follows,

$$H = \int d^3r \psi^\dagger(\mathbf{r}) \left[-\frac{\hbar^2}{2m} \nabla^2 + V(\mathbf{r}) - \bar{\mu} \right] \psi(\mathbf{r})$$

*Electronic address: jmh@seu.edu.cn

$$+\frac{g}{2} \int d^3r \psi^\dagger(\mathbf{r}) \psi^\dagger(\mathbf{r}) \psi(\mathbf{r}) \psi(\mathbf{r}) \quad (1)$$

where $\psi(\mathbf{r})$ and $\psi^\dagger(\mathbf{r})$ are the boson field operators for annihilating and creating an atom at site \mathbf{r} respectively; $g = 4\pi a_s \hbar^2/m$, where a_s is the s -wave scattering length, which is positive for atoms with repulsive interactions; m is the mass of atoms and $\bar{\mu}$ is the chemical potential; $V(\mathbf{r})$ is an external potential. In our model, the external potential $V(\mathbf{r})$ is a two-dimensional superlattice potential such as $V(x, y) = V_1 \cos^2(kx) \cos^2(ky) + V_2 [\cos^2(kx/2) \cos^2(ky/2) + \sin^2(kx/2) \sin^2(ky/2)]$, which is schematically displayed in FIG.1. This superlattice potential consists of two sublattices that we denote as sublattice ‘A’ and sublattice ‘B’ with the potential depths V_A and V_B , respectively. Such a two-dimensional superlattice can be built with optical techniques. For simplicity, we do not consider the shallow harmonic trapping potential, which is usually required in experiments to trap atomic gases.

In periodic potentials, the atomic states are represented by Bloch wave functions, which can be expanded in terms of a set of Wannier states that are well localized at lattice sites. Because of the translational symmetry of each sublattice, the Wannier function $w_i(\mathbf{r})$ is equal to $w_A(\mathbf{r} - \mathbf{R}_i)$ or $w_B(\mathbf{r} - \mathbf{R}_i)$ for sublattice A and B respectively, where \mathbf{R}_i is a lattice vector. At zero temperature, the atoms are in the lowest band states. Expanding the field operators in the lowest vibrational Wannier states as $\psi(\mathbf{r}) = \sum_i b_i w_i(\mathbf{r})$, Eq.(1) reduces to the extended Bose-Hubbard Hamiltonian,

$$H = -t \sum_i \left[b_{(i_x, i_y)}^\dagger b_{(i_x+1, i_y)} + b_{(i_x, i_y)}^\dagger b_{(i_x, i_y+1)} + \text{H.C.} \right] - \sum_i \mu_i n_i + \frac{1}{2} \sum_i U_i n_i (n_i - 1) \quad (2)$$

where (i_x, i_y) is the coordinate position of lattice site i in the two-dimensional optical superlattice. $b_{(i_x, i_y)}$ and $b_{(i_x, i_y)}^\dagger$ represent the operators for annihilating and creating an atom at lattice site $i = (i_x, i_y)$ respectively; $t = \int d\mathbf{r} w_A^*(\mathbf{r} - \mathbf{r}_i) [-\frac{\hbar^2}{2m} \nabla^2 + V(\mathbf{r})] w_B(\mathbf{r} - \mathbf{r}_j)$ is the tunnelling parameter between adjacent lattice sites in the different sublattices A and B. U_i is the repulsive on-site interaction between atoms at lattice site i ; μ_i is the effective chemical potential corresponding to lattice site i . In the two different sublattices, the effective chemical potential and the on-site interaction are

$$\begin{cases} \mu_i = \mu, U_i = U_A & \text{when } i_x + i_y \text{ is even,} \\ \mu_i = \mu - \delta, U_i = U_B & \text{when } i_x + i_y \text{ is odd,} \end{cases}$$

where $\mu = \bar{\mu} - \int d\mathbf{r} V(\mathbf{r}) |w_A(\mathbf{r})|^2$ and $\delta = \int d\mathbf{r} V(\mathbf{r}) (|w_B(\mathbf{r})|^2 - |w_A(\mathbf{r})|^2)$; $U_A = g \int d\mathbf{r} |w_A(\mathbf{r})|^4/m$ and $U_B = g \int d\mathbf{r} |w_B(\mathbf{r})|^4/m$ are the on-site interactions on the two different kinds of sublattice sites.

With Gutzwiller’s ansatz, we can write the wavefunctions of the system as[1],

$$|\Psi_G\rangle = \prod_i |\phi_i\rangle, \quad |\phi_i\rangle = \sum_n f_n^{(i)} |n\rangle_i, \quad (3)$$

where $|n\rangle_i$ is the Fock state with n particles at the lattice site i and $f_n^{(i)}$ are the variational parameters, which satisfy the normalized condition $\sum_n |f_n^{(i)}|^2 = 1$ for each lattice site i . To find the ground state of the system, we minimize the expectation value of the Hamiltonian(2), $\langle \Psi_G | H | \Psi_G \rangle$, with the variational parameters $\{f_n^{(i)}\}$, under a given chemical potential μ . In our work, we use conjugate gradient algorithm to minimize the expectation value of the Hamiltonian. The system contains 10×10 lattice sites and the truncated number of Fock states is 6. To eliminate the boundary effects, periodic boundary conditions are used.

To identify different quantum phases, we define the static structure factor as follows:

$$S(\mathbf{k}) = \frac{1}{N} \sum_{i,j} e^{i\mathbf{k} \cdot (\mathbf{R}_i - \mathbf{R}_j)} \langle n_i n_j \rangle \quad (4)$$

where \mathbf{R}_i is a lattice vector and N is the number of lattice sites. The diagonal long-range order and the off-diagonal long-range order in the system of ultracold bosonic atoms in a two-dimensional optical superlattice are measured by $S(\pi, \pi)$ and $\phi = \langle b \rangle$, respectively. The Mott-insulator phase is a state with particle number density pinned at an integer such as $n = 1, 2, \dots$, which corresponds to a commensurate filling of the lattice. The Mott-insulator phase is characterized by $S(\pi, \pi) = 0$ and $\phi = 0$. In the density wave phase, the particle number density is modulated by with the period of twice lattice constant and is pinned at two different integers in the two different sublattices. The density wave phase is a superlattice crystal with the diagonal long-range order measured by $S(\pi, \pi)$, and without the off-diagonal long-range order. Therefore, $S(\pi, \pi) \neq 0$ and $\phi = 0$ feature the density wave phase. In the supersolid phase, the diagonal long-range order and the off-diagonal long-range order coexist, so the supersolid phase is characterized by $S(\pi, \pi) \neq 0$ and $\phi \neq 0$. The superfluid phase, which is absent in our model, is characterized by $S(\pi, \pi) = 0$ and $\phi \neq 0$.

FIG. 2 shows the phase diagram of ultracold bosonic atoms in an optical superlattice for $U_B = 0.5U_A$ and $\delta = 0.2U_A$, which is obtained by solving the Hamiltonian (2) numerically with Gutzwiller approach. This phase diagram is a result of competition among the tunnelling term and the two different on-site interactions in the two different sublattices. From this figure, we can find that Mott-insulator, density wave and supersolid phases appear in some regimes of parameters, while the superfluid phase, which usually appears in optical lattice-cold atom systems, is absent in our model. The Mott-insulator and density wave phases are denoted as

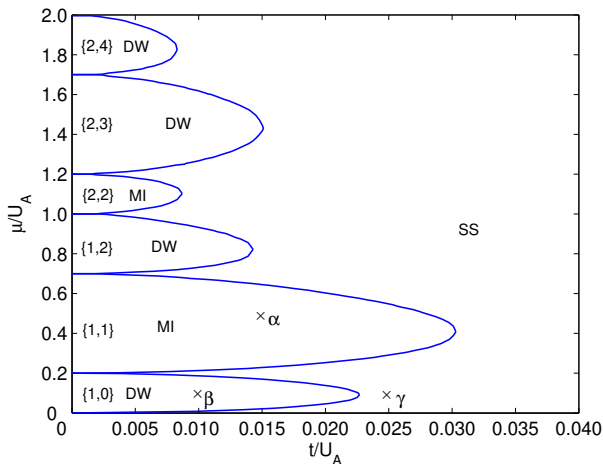


FIG. 2: Phase diagram of ultracold bosonic atoms in an optical superlattice for $U_B = 0.5U_A$ and $\delta = 0.2U_A$. t/U_A and μ/U_A are the dimensionless hopping matrix element and the chemical potential respectively. In this diagram, MI, DW and MI denote the Mott-insulator, density wave and supersolid phases respectively. $\{n_A, n_B\}$ represents the average particle density in sublattices A and B when the system is in MI or DW phase. The points marked with ‘x’, of which the first order correlation function and the second order correlation function are shown in FIG.3, are denoted by ‘ α ’, ‘ β ’, and ‘ γ ’.

$\{n_A, n_B\}$ for their filling numbers in the sublattice A and B. The second and fourth lobes counted from the bottom, denoted as $\{1, 1\}$ and $\{2, 2\}$ respectively, belong to the Mott-insulator phase. For the Mott-insulator phase $\{1, 1\}$, the critical value of t/U_A for the MI-SS phase transition is 0.031, while the corresponding value of the MI-SF transition in a two-dimensional optical lattice is 0.043[1]. Thus, the Mott-insulator phase is more unstable in optical superlattice than in optical lattice due to competition between the different on-site interactions in the different sublattice in the optical superlattice. The first, third, fifth and sixth lobes, denoted as $\{1, 0\}$, $\{1, 2\}$, $\{2, 3\}$ and $\{2, 4\}$ respectively, belong to the density wave phase. The reason that the density wave phase $\{1, 0\}$ appears is the difference of the effective chemical potentials for the two different sublattice, while the other density wave lobes are the result of competition among the tunnelling term and the two on-site interaction in the two sublattices. The other regime except the Mott-insulator and density wave lobes, where the diagonal long-range order and the off-diagonal long-range order appear simultaneously, belongs to the supersolid phase. In our model, we do not find the superfluid phase, which conventionally appears in the optical lattice-cold atom system[1, 2].

The techniques to detect the quantum phases which we find in the system of ultracold bosonic atoms in our model are accessible for now. Altman *et al.* have proposed to utilize shot-noise correlations to probe complex many-body states of trapped ultracold atoms, e.g.,

Mott states[16]. Scarola *et al.* have suggested to use the noise-correlation technique to detect the supersolid phase of cold atoms with long-range dipolar interactions in an optical lattice[17]. The correlations for the case of a bosonic Mott insulating state[18], anticorrelations for the case of a fermionic band insulating state[7], and the pair-correlated atoms created by dissociating weakly bound diatomic molecules near a Feshbach resonance[19] have recently been observed through shot-noise correlations techniques experimentally.

For the time of flight detection, the atoms interact weakly after the trapped optical lattice is adiabatically turned off, and the number of atoms at position \mathbf{r} in the expanding cloud after a time T is given by $\langle n(\mathbf{r}) \rangle_T \approx |\tilde{w}(\mathbf{k}(\mathbf{r}))|^2 \rho_0(\mathbf{k}(\mathbf{r}))$, where \tilde{w} is the Fourier transform of the Wannier function[16, 17]. The relation between the lattice momentum and the position in the expanding cloud after an expanding time T is $\mathbf{k}(\mathbf{r}) = a_0 m \mathbf{r} / \hbar T$, where m is the mass of atom and a_0 is the width of the Wannier state in the lattice. ρ_0 is a first order correlation function in the lattice momentum space which is defined as follows,

$$\rho_0(\mathbf{k}) = \sum_{i,j} e^{i\mathbf{k} \cdot (\mathbf{R}_i - \mathbf{R}_j)} \langle b_i^\dagger b_j \rangle, \quad (5)$$

where \mathbf{R}_i is a lattice vector. The first order normalized correlation function is defined as $\rho(\mathbf{k}) \equiv \rho_0(\mathbf{k})/N$, where N is the number of lattice sites. The shot-noise correlation function in the expanding atomic cloud after an expanding time T is $\mathcal{G}(\mathbf{r}, \mathbf{r}') = \langle n(\mathbf{r})n(\mathbf{r}') \rangle_T - \langle n(\mathbf{r}) \rangle_T \langle n(\mathbf{r}') \rangle_T$, which is proportional to momentum correlations in the ground state of the optical lattice trapped system,

$$\mathcal{G}(\mathbf{r}, \mathbf{r}') \sim |\tilde{w}(\mathbf{k}(\mathbf{r}))|^2 |\tilde{w}(\mathbf{k}(\mathbf{r}'))|^2 G_0(\mathbf{k}(\mathbf{r}), \mathbf{k}(\mathbf{r}')), \quad (6)$$

where $G_0(\mathbf{k}, \mathbf{k}')$ is the second order correlation function in the lattice momentum space. the second order normalized correlation function is defined by $G(\mathbf{k}, \mathbf{k}') = G_0(\mathbf{k}, \mathbf{k}') / \rho_0(\mathbf{k}) \rho_0(\mathbf{k}')$, which can be written as [17],

$$G(\mathbf{k}, \mathbf{k}') = \frac{\sum_{ii'jj'} e^{i\mathbf{k} \cdot (\mathbf{R}_i - \mathbf{R}_{i'}) + i\mathbf{k}' \cdot (\mathbf{R}_j - \mathbf{R}_{j'})} \langle b_i^\dagger b_{j'}^\dagger b_j b_{i'} \rangle}{\rho_0(\mathbf{k}) \rho_0(\mathbf{k}')} - 1 + \frac{ma_0}{\hbar T} \frac{\delta(\mathbf{k} - \mathbf{k}')}{|\tilde{w}(\mathbf{k}')|^2 \rho_0(\mathbf{k}')}, \quad (7)$$

where the $\delta(\mathbf{k} - \mathbf{k}')$ term is the autocorrelation term and will be dropped in the subsequent discussion because it only contributes to the second order correlation function for $\mathbf{k} = \mathbf{k}'$ and does not contain the characterizing information about the correlation function distribution in the momentum space.

To identify the quantum phases, such as the Mott-insulator, density wave and supersolid phases, in experiments, we pick out three points α, β and γ , representing the three quantum phases respectively, from the phase

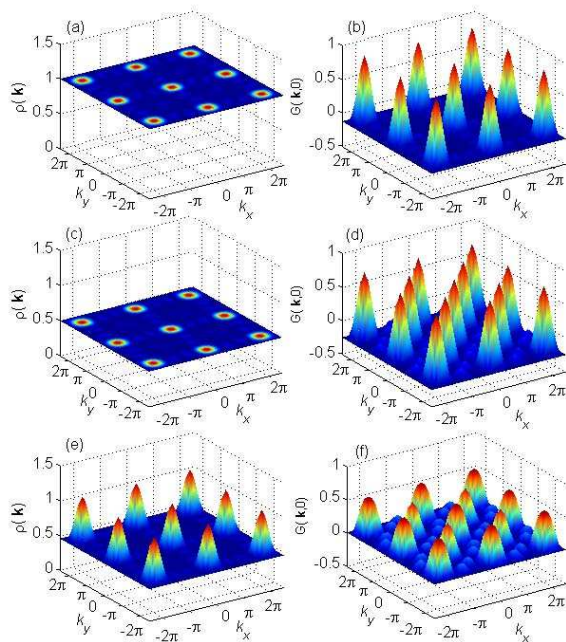


FIG. 3: (color online). The first order and the second order normalized density correlations of different quantum phases as functions in the lattice momentum space. (a) and (b) are respectively the first order and the second order normalized density correlations in the lattice momentum space of a Mott-insulator phase at the point denoted by ‘ α ’ in FIG.2. (c) and (d) are respectively the first order and the second order normalized density correlations in the lattice momentum space of a density wave phase at the point denoted by ‘ β ’ in FIG.2. (e) and (f) are respectively the first order and the second order normalized density correlations in the lattice momentum space of a supersolid phase at the point denoted by ‘ γ ’ in FIG.2.

diagram shown in FIG.2. For the three picked points, we calculate the distributions of $\rho(\mathbf{k})$ and $G(\mathbf{k},0)$ in the lattice momentum space, which are shown in FIG. 3. For the Mott-insulator phase, the first order normalized correlation function is almost a constant and the second order normalized correlation function has peaks at points $(0,0)$ and $(\pm 2\pi, \pm 2\pi)$ in the lattice momentum space. For the density wave phase, the first order normalized correlation function is almost a constant and the normalized second order correlation function has peaks at points $(0,0)$, $(\pm\pi, \pm\pi)$ and $(\pm 2\pi, \pm 2\pi)$ in the lattice momentum space. For the supersolid phase, the first order normalized correlation has peaks at points $(0,0)$ and $(\pm 2\pi, \pm 2\pi)$ and the second order normalized correlation function has peaks at points $(0,0)$, $(\pm\pi, \pm\pi)$ and $(\pm 2\pi, \pm 2\pi)$ in the lattice momentum space. These characterizing features of correlation functions in the lattice momentum space can be detected by probing the correlations in the coordinate space of the atomic cloud after an expanding time T with the time-of-flight and noise-correlation techniques.

In our work, for simplicity, we do not consider the shallow harmonic trapping potential, which is usually required to trap atomic gases in the practical experiments. In fact, the presence of a shallow harmonic trapping potential does not change the intrinsic features that we have discussed. The energy offset due to the shallow harmonic trapping potential can be combined in the effective chemical potential. Thus, the effective chemical potential varies with the position, so the phase separation may occur in the practical experiments. For the time-of-flight and noise-correlation detections, in the practical experiments where the shallow harmonic trapping potential exists, we may obtain lower peaks at the edge points than at the center in the expanding atomic cloud.

In summary, we have investigated the quantum phases of ultracold bosonic atoms in an two-dimensional optical superlattice. First, we derived the extended Bose-Hubbard Hamiltonian without nearest-neighbor interactions, which are conventionally required to manifest a supersolid phase. In our model, through solving the extended Bose-Hubbard Hamiltonian with Gutzwiller approach we found that the supersolid and the density wave phases, addition to the Mott-insulator phase, appear, while the superfluid phase vanishes. The detection of these quantum phases with the time-of-flight and noise-correlation techniques was proposed. We have calculated the first order and second order correlation functions for different quantum phases and discussed their differences to distinguish them in experiments.

This work was in part supported by NSF of China Grant No. 10571091.

-
- [1] D. Jaksch *et al.*, Phys. Rev. Lett. 81, 3108(1998).
 - [2] M. Greiner *et al.*, Nature 415, 39 (2002).
 - [3] B. Paredes, *et al.*, Nature 429, 277 (2004); T. Stöferle *et al.*, Phys. Rev. Lett. 92, 130403 (2004).
 - [4] L. Fallani *et al.*, Phys. Rev. Lett. 98, 130404 (2007).
 - [5] K. Winkler *et al.*, Nature 441, 853 (2006).
 - [6] M.W. Zwierlein *et al.*, Nature 442, 54(2006); J. K. Chin *et al.*, Nature 443, 961 (2006); M. Köhl *et al.*, Phys. Rev. Lett. 94, 080403 (2005); T. Stöferle *et al.*, Phys. Rev. Lett. 96, 030401 (2006).
 - [7] T. Rom *et al.*, Nature 444, 733 (2006).
 - [8] K. Günter *et al.*, Phys. Rev. Lett. 96, 180402 (2006); S. Ospelkaus *et al.*, Phys. Rev. Lett. 96, 180403 (2006).
 - [9] D. Jaksch *et al.*, Phys. Rev. Lett. 82, 1975 (1999); G. K. Brennen *et al.*, Phys. Rev. Lett. 82, 1060 (1999); J. K. Pachos and P. L. Knight, Phys. Rev. Lett. 91, 107902 (2003).
 - [10] A. F. Andreev and I. M. Lifshitz, Sov. Phys. JETP 29, 1107 (1969); G. Chester, Phys. Rev. A 2, 256 (1970); A. J. Leggett, Phys. Rev. Lett. 25, 1543 (1970).
 - [11] E. Kim and M. H. W. Chan, Science 305, 1941 (2004).
 - [12] K. Góral *et al.*, Phys. Rev. Lett. 88, 170406 (2002); A. van Otterlo *et al.*, Physical Rev. B 52, 16176 (1995); P. Sengupta *et al.*, Phys. Rev. Lett. 94, 207202 (2005); D.

- L. Kovrizhin *et al.*, Europhys. Lett. 72, 162 (2005).
- [13] V. W. Scarola and S. Das Sarma, Phys. Rev. Lett. 95, 033003 (2005).
- [14] H. P. Büchler and G. Blatter, Phys. Rev. Lett. 91, 130404 (2003).
- [15] S. Wessel and M. Troyer, Phys. Rev. Lett. 95, 127205 (2005); R. G. Melko *et al.*, Phys. Rev. Lett. 95, 127207 (2005); D. Heidarian and K. Damle, Phys. Rev. Lett. 95, 127206 (2005).
- [16] E. Altman *et al.*, Phys. Rev. A 70, 013603(2004).
- [17] V. W. Scarola *et al.*, Phys. Rev. A 73, 051601(R) (2006).
- [18] S. Fölling *et al.*, Nature, Vol 444, 733(2006).
- [19] M. Greiner *et al.*, Phys. Rev. Lett. 94, 110401(2005).